Proceedings of the Korean Nuclear Society Autumn Meeting
Seoul, Korea, October 1999

Photoproton Reaction Cross Sections Involving ^{16}O up to 120 MeV in the Continuum Random Phase Approximation

Jeong-Yeon Lee, Young-Ouk Lee, and Jongwha Chang
Korea Atomic Energy Research Institute
P. O. Box 105, Yusung, Taejon 305-600, Korea

Abstract

The total and 90° differential cross sections for the photoproton reactions $^{16}\mathrm{O}(\gamma,p)^{15}\mathrm{N}$ leading to the ground and third excited states of ^{15}N are calculated for photon energies up to 120 MeV within the continuum random phase approximation (CRPA) approach taking into account particle-hole correlations and the spreading (damping) effects as well as the continuum state boundary condition. In solving the continuum response function, a correlated source function which makes the numerical calculation possible is used. The structures of the theoretical cross sections are in good agreement with the corresponding experimental data.

I Introduction

The photon is an ideal probe of a nuclear structure as the electromagnetic interaction is well understood and weak so that the nucleus is only mildly perturbed. Thus in principle precise structure information may be extracted from photonuclear reaction data. The low energy photoabsorption is an ideal tool to study the isovector giant dipole resonance (GDR) since it selectively excites ΔT=1 and ΔL=1 excitations [1]. The intermediate energy photonuclear reactions are known to probe short-range interactions not only from nucleon-nucleon correlations but also from exchange currents [2, 3].

The giant resonance (GR) of nuclei has always been of central interest in photonuclear reaction studies. The random phase approximation (RPA) theory [4–8] works well in reproducing the position and the strength of the GR of low multipolarity. A nucleus is excited primarily through particle-hole (ph) excitations in an external field, say, hadron or electron inelastic scattering. The interaction between particles and holes produces correlations between the ph pairs, which play an important role in determining the characteristics of the energy spectrum [9]. The GR states are described as highly correlated superpositions of single ph excitations out of a closed shell. However, the RPA calculations are not able to predict the widths of the states

because the states are treated as discrete ones even in the continuum and because the particle damping effect is overlooked.

In recent years, a method to calculate the nuclear response in the continuum by an external field has been proposed [10]. In this method the strength function is calculated within the continuum random phase approximation (CRPA) taking into account *ph* correlations and the spreading (damping) effects as well as the continuum boundary condition. A correlated source function is introduced to take care of continuum states. The iterative Lanczos method is adopted for solving large-scale inhomogeneous coupled-channels (CC) integral equations for excited particles. The spreading (damping) effects are considered by introducing a complex optical potential for the excited particles. This method includes both reaction part and structure part simultaneously, while most of the former methods [4, 9] describe both parts separately. This theory has been quite successful in explaining GR's induced by hadron inelastic scattering [11–13] or electron inelastic scattering [14] and in describing Δ-excitations in nuclei [15, 16].

A lot of experimental [17–23] and theoretical [4, 5, 8, 24–27] works for the ^{16}O photonucleon reactions leading to ground states of ^{15}N and ^{15}O, that is, $^{16}\mathrm{O}(\gamma, p_0)^{15}\mathrm{N}$ and $^{16}\mathrm{O}(\gamma, n_0)^{15}\mathrm{O}$ have been reported. However, few works for the photonucleon reactions leading to the excited states have been reported.

An early experiment for the photoproton reaction $^{16}\mathrm{O}(\gamma, p_3)^{15}\mathrm{N}^*(6.324$ MeV) leading to the third excited state with $3/2^-$ in ^{15}N has been done by Morrison [28] in the GDR region. Later, an experiment for the reaction over the wide energy range from the threshold up to 120 MeV has been performed by Khodjachikh *et al.* [29] using a technique of a diffusion chamber in a magnetic field. In the experimental cross section, besides the GDR peak at E_γ= 22 MeV another resonance peak was observed at E_γ= 35 MeV making a deep minimum at 29 MeV.

The calculations of the total and 90^o differential cross sections for the reaction $^{16}\mathrm{O}(\gamma, p_3)^{15}\mathrm{N}^*$ have been carried out by Buck and Hill (BH) [24] based on the Tamm-Dancoff approximation (TDA) involving the calculations of the continuum state. The calculations were performed in the GDR region only and the numerical results were concerned only with the component of complete wave function which has $J^\pi = 1^-$. Therefore, it was not fully understood how the $3/2^-$ state of ^{15}N is formed *via* the photoproton reaction. And up to the present time no comparable experiments and theories of the photoproton reaction have been reported.

The present research aims for a theoretical description of photoproton reactions involving ^{16}O leading to the ground and third excited states of ^{15}N by using the CRPA approach in the photon energies up to 120 MeV.

II CRPA Formalism for Photonuclear Reactions

The total photoabsorption cross section due to the electric λ-pole in the $A(\gamma, p)B$ reaction may be given as [12, 13]

$$\sigma_\lambda = \frac{(2\pi)^3(\lambda+1)}{\lambda[(2\lambda+1)!!]^2} k_\gamma^{2\lambda-1} S_\lambda, \tag{1}$$

where k_γ is the wave number of the absorbed photons. If the target is assumed to be a spherical nucleus, then the strength function S_λ can be written as [10]

$$S_\lambda = \mathrm{Im} \sum_{ph} [- \frac{1}{\pi} \langle \rho_{ph} \, |G| \, \rho_{ph} \rangle], \tag{2}$$

where

$$\rho_{ph} = (y_p | e r^\lambda Y_{\lambda\mu}(\hat{\mathbf{r}}) | \phi_{\tilde{h}} \rangle . \tag{3}$$

Here, y_p is the spin-angle wave function for particle p while $\phi_{\tilde{h}}$ denotes the hole wave function of $\tilde{h}$ which is the time reversal state of the hole h. The symbol $(\, | \, | \, \rangle$ in Eq. (3) indicates that the integrals are carried out only over the spin-angle variables. G in Eq. (2) is the ph Green's function of the target system,

$$G = \frac{1}{E - H_h - H_p - V_{ph} + i\varepsilon}, \tag{4}$$

where the excitation energy, E, of the system is positive for the forward amplitude and negative for the backward amplitude in the RPA. H_h is the Hamiltonian for the hole nucleus, and H_p is the Hamiltonian for the excited particle p containing a complex optical potential U_p. V_{ph} is the effective ph interaction which is responsible for the ph correlations.

To obtain the $G|\rho_{ph} \rangle$ in Eq. (2) Λ_{ph} is defined by

$$|\Lambda_{ph} \rangle = |\rho_{ph} \rangle + V_{ph} G_0 |\Lambda_{ph} \rangle , \tag{5}$$

where Λ_{ph} is the so-called correlated source function and is localized only in the nuclear region even for continuum states. G_o is the free Green's function without the effective ph interaction V_{ph}. The inhomogeneous CC integral equation of Eq. (5) is the basic equation to solve. For solving Eq. (5), we adopt the iterative Lanczos method [30], which has been extensively used in the past for large shell-model calculations.

The strength function, S_λ, then becomes

$$S_\lambda = \mathrm{Im} \sum_{ph} [- \frac{1}{\pi} \langle \rho_{ph} | G_0 | \Lambda_{ph} \rangle]. \tag{6}$$

S_λ may be decomposed into two components, $S_\lambda^\downarrow$ and $S_\lambda^\uparrow$: $S_\lambda^\downarrow$ describes the contribution from the damping (spreading) process, *i.e.*, the particle absorption due to W_p in U_p, while $S_\lambda^\uparrow$ is due to direct knockout by photoabsorption. Following the technique used to derive the knockout-fusion cross-section formula [31], $S_\lambda^\downarrow$ can be written as

$$S_\lambda^\downarrow = - \langle G_0 \Lambda_{ph} | W_p | G_0 \Lambda_{ph} \rangle . \tag{7}$$

The $S_\lambda^\uparrow$ may then be obtained by

$$S_\lambda^\uparrow = \sum_h \int \frac{\mathrm{d}^2 \sigma_B}{\mathrm{d}E_p \mathrm{d}\Omega_p} \mathrm{d}\Omega_p, \tag{8}$$

where the knockout cross section can be calculated by

$$\frac{\mathrm{d}^2\sigma_B}{\mathrm{d}E_p\mathrm{d}\Omega_p} = \frac{m_p k_p}{(2\pi)^3\hbar^2}|\langle\ \chi_p|\Lambda_{ph}\ \rangle|^2, \tag{9}$$

χ_p being the distorted wave function of the knocked-out particle p against the residual nucleus B.

The photoabsorption cross section is then

$$\sigma_\lambda(\gamma,p) = \frac{(2\pi)^3(\lambda+1)}{\lambda[(2\lambda+1)!!]^2}k_\gamma^{2\lambda-1}S_\lambda^{\uparrow}, \tag{10}$$

and the angular distribution of the photoabsorption cross section is

$$\frac{\mathrm{d}\sigma_\lambda(\gamma,p)}{\mathrm{d}\Omega_p} = \frac{(2\pi)^3(\lambda+1)}{\lambda[(2\lambda+1)!!]^2}k_\gamma^{2\lambda-1}\frac{\mathrm{d}^2\sigma_B}{\mathrm{d}E_p\mathrm{d}\Omega_p}. \tag{11}$$

III Application

The CRPA method is applied to the GR states in ^{16}O induced by photoproton reactions $^{16}\mathrm{O}(\gamma,p)^{15}\mathrm{N}$ leading to the ground and third excited states. Consider the photoproton reaction processes. Initially, ^{16}O is in the ground state whose shell structure is assumed to be $(1s_{\frac{1}{2}})^2(1p_{\frac{3}{2}})^4(1p_{\frac{1}{2}})^2$ for both protons and neutrons. However, with an absorbing of photons, a proton in the $1p_{\frac{3}{2}}$ or $1p_{\frac{1}{2}}$ state is promoted to an excited state, leaving a hole in the $1p_{\frac{3}{2}}$ or $1p_{\frac{1}{2}}$ state for the reactions leading to the ground and third excited states, respectively, thus making a ph configuration. The excited particle may be in the bound state as in $1d_{\frac{5}{2}}$, and $2s_{\frac{1}{2}}$ or above the particle threshold as in continuum states $1d_{\frac{3}{2}}$, $1f_{\frac{7}{2}}$, $2p_{\frac{3}{2}}$, $1f_{\frac{5}{2}}$, $2p_{\frac{1}{2}}$, etc. ph configurations which correspond to particular transitions leading to the ground and third excited states are denoted as arrow in Fig. 1 and Fig. 2, respectively. The GR states are explained as superpositions of such ph configurations.

For the hole Hamiltonian, H_h, in Eq. (4), a local potential of the Woods-Saxon form is assumed. The radius parameter and the diffuseness parameter for the nucleus are taken to be 1.25 fm and 0.53 fm, respectively, in all cases, which are the same as ones of BH [24]. However, the depths for the real and the spin-orbit potentials are chosen to be -58.2 MeV and -9.89 MeV, respectively, for all single particles in ^{16}O, thus satisfying the orthogonality condition. (In the calculation of BH, the different potential parameters are used for each single particle in ^{16}O.) The calculated single-particle energy level scheme for the ^{16}O is shown in Fig. 1 and Fig. 2 with the ph configurations.

The potentials for the excited particles are taken to be the usual optical potentials: a real potential with a Woods-Saxon shape, an imaginary absorption potential peaked near the nuclear surface, a spin-orbit potential, and a Coulomb potential given by

$$U_p(r) = \frac{V}{1+e^{x_v}} + \frac{4iWe^{x_w}}{(1+e^{x_w})^2} + V_{so}\Big[\frac{\hbar}{m_\pi c}\Big]^2\frac{1}{a_{so}r}\frac{e^{x_{so}}}{(1+e^{x_{so}})^2}\,\boldsymbol{\ell}\cdot\boldsymbol{\sigma} - C(r) \tag{12}$$

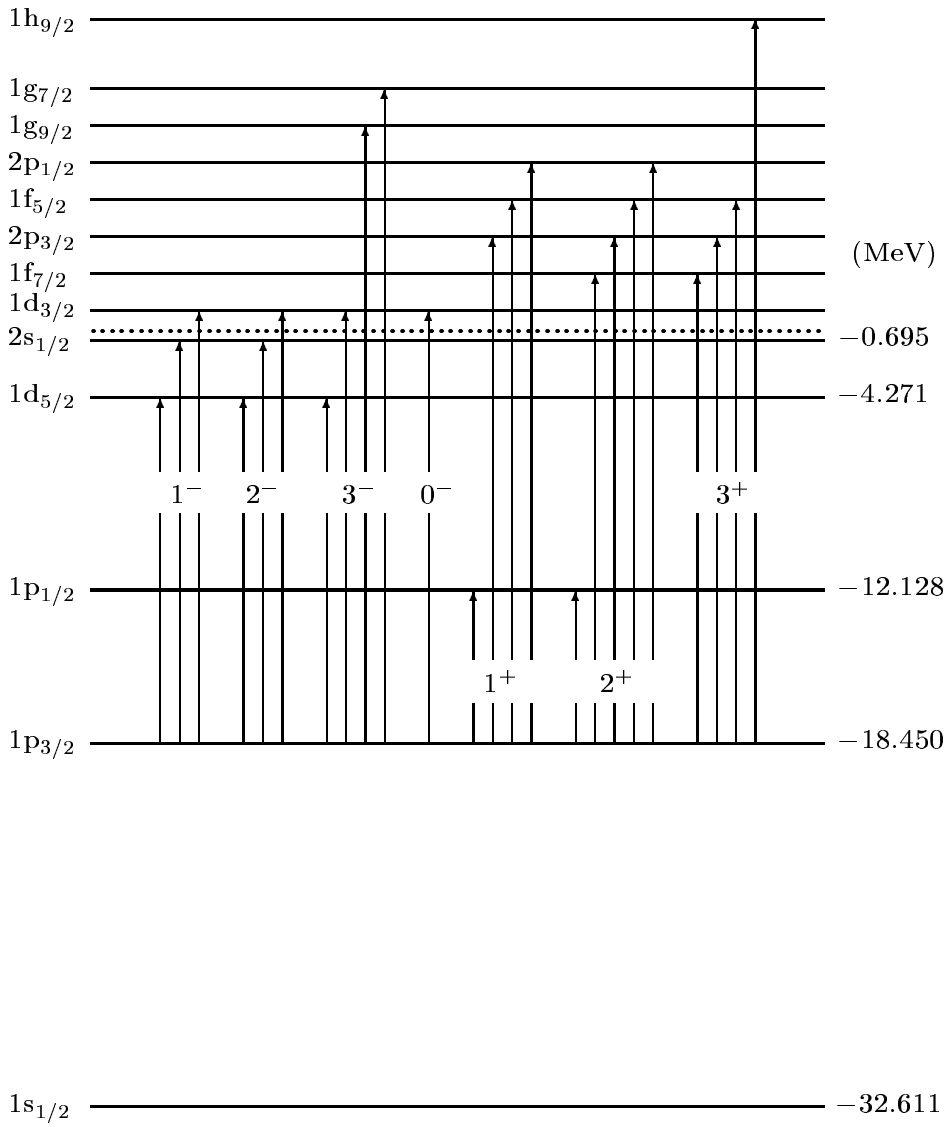

Figure 1: Calculated single proton energy levels in ^{16}O. Each arrow denotes a *ph* configuration for the corresponding transition leading to the $3/2^-$ excited state of ^{15}N.

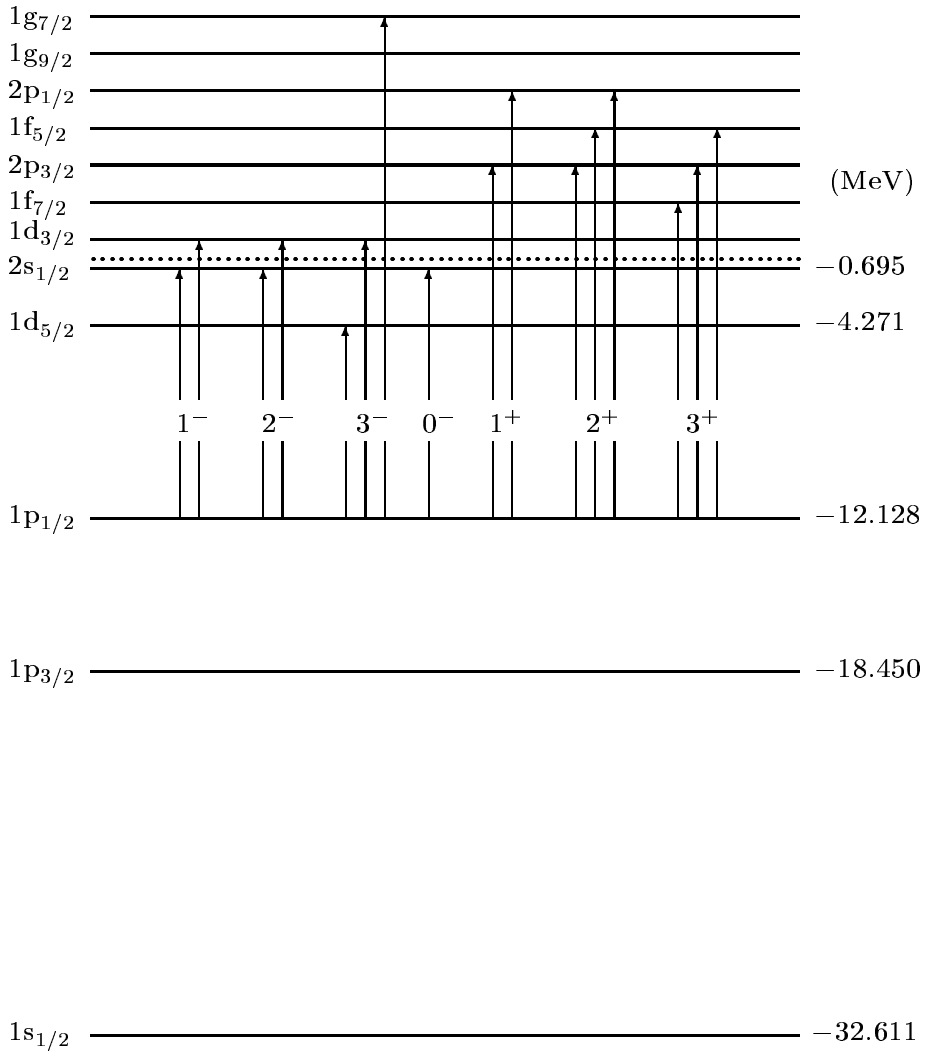

Figure 2: Calculated single proton energy levels in ^{16}O. Each arrow denotes a *ph* configuration for the corresponding transition leading to the ground state of ^{15}N.

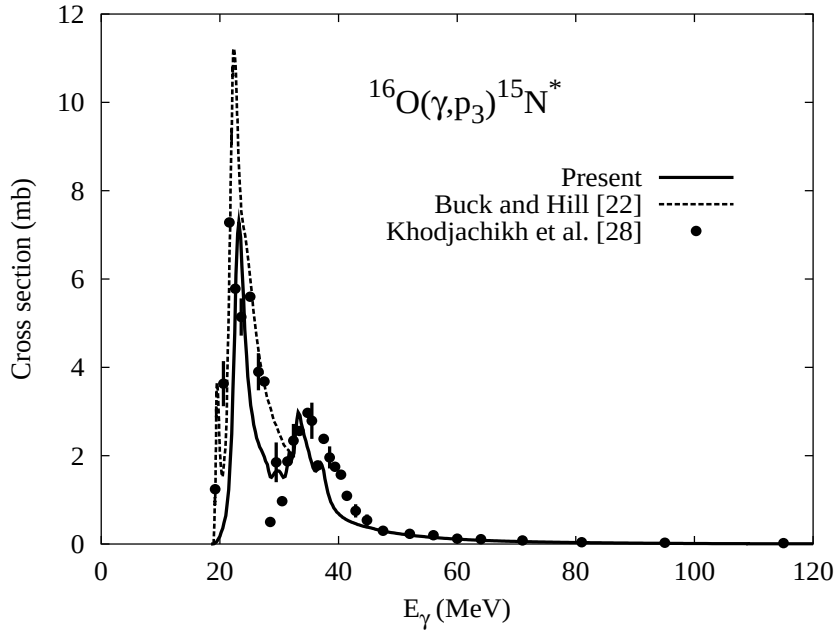

Figure 3: The theoretical cross sections of the photoproton reaction $^{16}\mathrm{O}(\gamma, p_3)^{15}\mathrm{N}^*(6.324\ \mathrm{MeV})$ leading to the $3/2^-$ excited states of ^{15}N compared with the calculated result by Buck and Hill [21] and the experimental data [26].

with

$$x_i = \frac{r - R_i}{a_i}, \quad R_i = r_i(A-1)^{\frac{1}{3}} \quad (i = v, w, so) \tag{13}$$

for a target nucleus of mass number A and $C(r)$ is the Coulomb potential. The diffuseness parameter a_i and radius parameter r_i are taken to be 0.53 fm and 1.25 fm, respectively, in all cases, which are used by BH. For the potential depths, V=−76.0 MeV, W=−0.74 MeV, and V_{so}=−9.8 are chosen.

If δ-function [32] is assumed, the residual interaction $V_{ph}(\mathbf{r_1}, \mathbf{r_2})$ may be given as [12, 13]

$$V_{ph}(\mathbf{r_1}, \mathbf{r_2}) = V_p \delta(\mathbf{r_1} - \mathbf{r_2})[a + bP_\sigma], \tag{14}$$

where P_σ is the spin exchange operator and $a + b = 1$. V_p is an interaction strength parameter taken to be -375.5 MeV·fm^3, and $[a + bP_\sigma = 0.7{+}0.3P_\sigma]$ is the exchange mixture, which is the zero-range version of the interaction used by BH [24].

First, the calculation of the total cross section for the reaction $^{16}\mathrm{O}(\gamma, p_3)^{15}\mathrm{N}^*$ leading to the third excited state of ^{14}N is performed within the CRPA approach in the energy region $0 \leq E_\gamma \leq$120 MeV. In Fig. 3, the calculated result for the reaction is compared with the experimental data of Khodjachikh *et al.* [29] and the calculated result by BH. Our theoretical result shows two main resonance peaks whose positions and strengths are in good agreement with the experimental results.

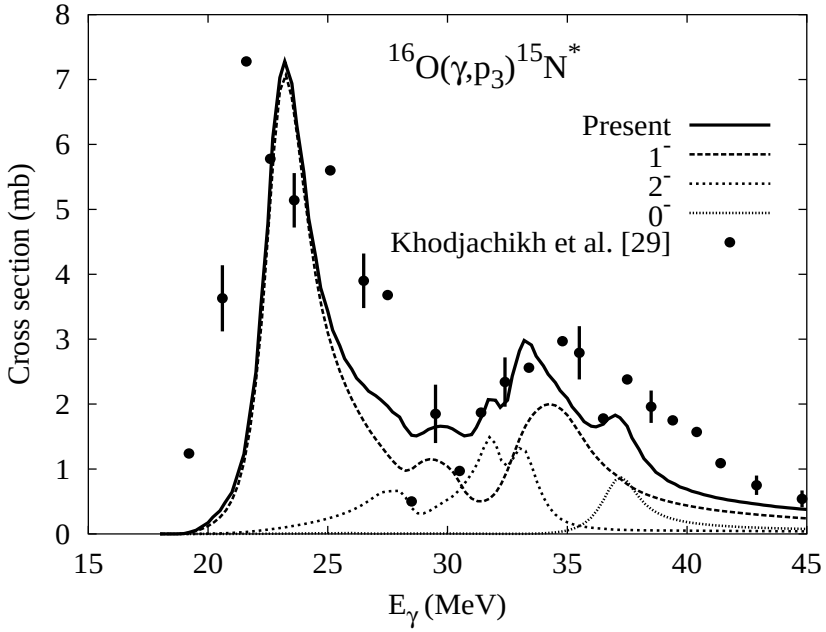

Figure 4: Enlarged plot of the theoretical and experimental [29] cross sections for the $^{16}\mathrm{O}(\gamma, p_3)^{15}\mathrm{N}^*(6.324$ MeV) reaction. Also shown are the partial wave decompositions of the cross section for each J^π.

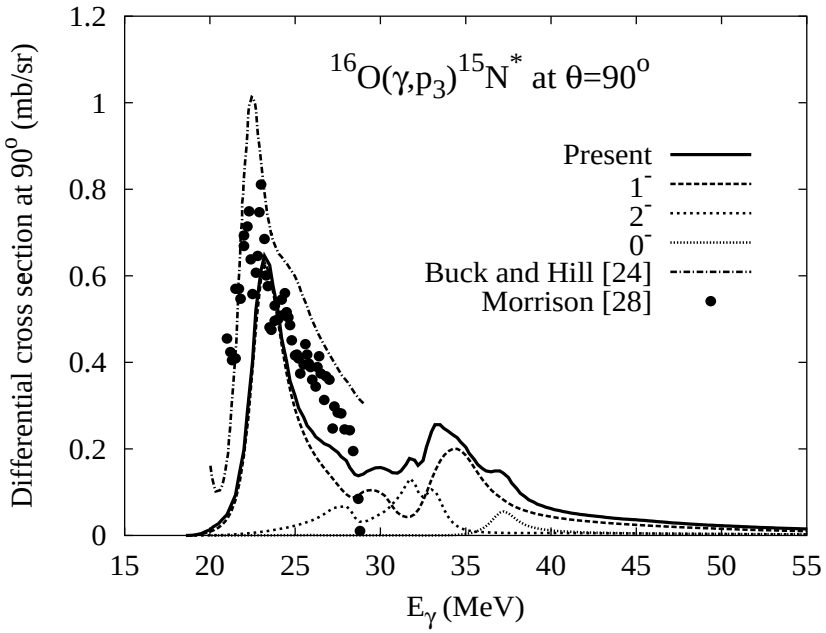

Figure 5: Comparison of theory and experiment [28] for the 90^o differential cross section of the photoproton reaction $^{16}\mathrm{O}(\gamma, p)^{15}\mathrm{N}^*$ leading to the third excited state with $3/2^-$ of ^{15}N. The calculated result by Buck and Hill [24] is also shown to be compared with out result.

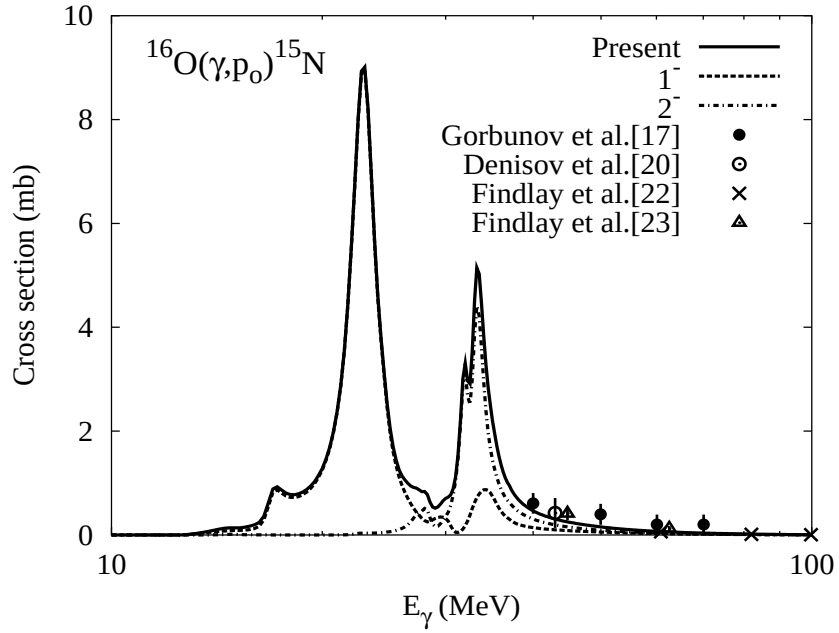

Figure 6: The theoretical cross sections of the photoproton reaction $^{16}\mathrm{O}(\gamma, p_o)^{15}\mathrm{N}$ leading to the ground state of ^{15}N compared with the experimental data [17,20,22,23]. Also shown are the partial wave decompositions of the cross section for each J^π.

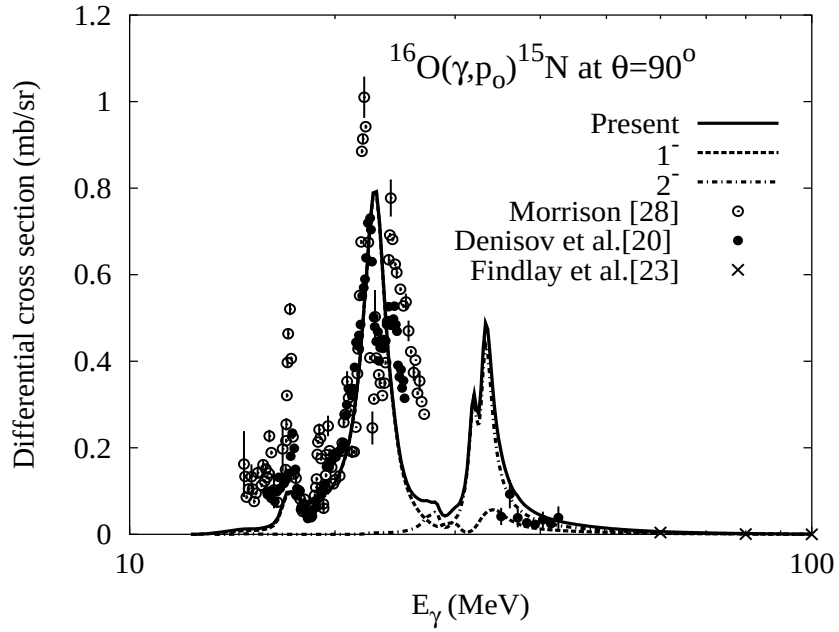

Figure 7: Comparison of theory and experiments [20,23,28] for the 90^o differential cross section of the photoproton reaction $^{16}\mathrm{O}(\gamma, p_o)^{15}\mathrm{N}$ leading to the ground state with $1/2^-$ of ^{15}N. Also shown are the partial wave decompositions of the cross section for each J^π.

Enlarged plots of the $^{16}O(\gamma, p_3)^{15}N^*$ reaction cross sections in the energy region $15 \leq E_\gamma \leq 45$ MeV are shown in Fig. 4 involving the partial cross sections for each total angular momentum and parity state J^π. The contributions from the 1^-, 2^-, and 0^- transitions which have negative parities are dominant over the region, while the contributions from the 1^+, 2^+, 3^+, and 3^- are small and negligible. The first resonance peak originates mainly from the contribution of 1^- transition, while for the second resonance peak, not only 1^- but also 2^- and 0^- transitions contribute to the cross section. The narrowness of the calculated widths compared with the experimental one [29] can be understood as the experimental $3/2^-$ excited state production cross section was simply obtained by subtracting the known ground state production cross section and the derived $1/2^+$ excited state production cross section from the total reaction cross section only. Khodjachikh *et al.* [29] also have mentioned that a deep minimum at 29 MeV in their experiment might be due to the bad resolution.

In Fig. 5, the calculated differential cross section at 90^o for the reaction $^{16}O(\gamma, p_3)^{15}N^*$ is compared with the corresponding experimental data of Morrison [28]. We find a reasonable agreement both in shape and in magnitude in the GDR region. The partial cross sections for each J^π are also shown. An aspect of the contributions from the J's is the same as for the cross section shown in Fig. 4. It is confirmed that the 1^- transition is dominant process for the first resonance peak, while the second resonance peak originates from not only 1^- but also 2^- and 0^- transition. The contributions from the 1^+, 2^+, 3^+, and 3^- are negligible. For the energy region above GDR region, more experiments are needed to be compared with our theoretical result.

The calculation of the total cross section for the photoproton reaction $^{16}O(\gamma, p_o)^{15}N$ leading to the ground state of ^{15}N is also performed within the CRPA approach. Figure 6 shows the theoretical cross sections of the $^{16}O(\gamma, p_o)^{15}N$ reaction compared with the experimental data [17, 20, 22, 23]. Also shown are the partial wave decompositions of the cross section for each J^π leading to the ground state. It is presented that the 1^- transition is the dominant process for the first resonance peak, while the second resonance peak originates from not only 1^- but also 2^- transition. The contributions from the 1^+, 2^+, 3^+, 0^-, and 3^- are small and negligible. For the GDR region, more experiments are needed to be compared with our theoretical result.

In Fig. 7, the calculated differential cross section at 90^o for the reaction $^{16}O(\gamma, p_o)^{15}N$ is compared with the experimental ones [20, 23, 28]. The partial wave decompositions of the cross section for each J^π are also shown. It is presented that the 1^- transition is the dominant process for the first resonance peak, while the second resonance peak originates from 1^- and 2^- transitions. The calculations for the partial cross sections from 1^+, 2^+, 3^+, 0^-, and 3^- are also performed. However, the contributions to the cross section are small and negligible.

IV Conclusions

The total and 90° differential cross sections for the photoproton reactions $^{16}O(\gamma,p)^{15}N$ leading to the ground and third $3/2^-$ excited states are calculated for photon energies up to 120 MeV using the CRPA approach taking into account ph correlations and the spreading (damping) effect as well as the continuum state boundary condition. In this calculation, the continuum response functions are reasonably solved by introducing the correlated source function and not only 1^- but also higher order of transitions are involved. It is shown that for the reaction $^{16}O(\gamma,p_3)^{15}N$ the first resonance peak is from the contribution of 1^- transition and the second one is from not only 1^- but also 2^- and 0^- transitions, while for the reaction $^{16}O(\gamma,p_o)^{15}N$ the first and second resonance peaks are from the contribution of 1^- transition and from 1^- and 2^- transitions, respectively. The CRPA theory gives results in overall agreement with the experimental data for the photoproton reactions $^{16}O(\gamma,p)^{15}$ leading to the ground and third excited states. Therefore, it is concluded that the photoproton reactions for the system ^{16}O in the energy region $0 \leq E_\gamma \leq 120$ MeV can be explained as a collective process dominated by $1p-1h$ states.

Acknowledgements

This work is supported by the Korea Ministry of Science and Technology as one of the long-term nuclear R&D programs.

References

[1] A. van der Woude, *Electric and Magnetic Giant Resonances in Nuclei*, edited by J. Speth (World Scientific, Singapore, 1991).

[2] B. Höistad, E. Nilsson, J. Thun, S. Dahlgren, S. Isaksson, G. S. Adams, C. Landberg, T. B. Bright, and S. R. Cotanch, Phys. Lett. B **276**, 294 (1992).

[3] G. S. Adams *et al.*, Phys. Rev. C **38**, 2771 (1988).

[4] S. Shlomo and G. F. Bertsch, Nucl. Phys. **A243**, 507 (1975).

[5] G. F. Bertsch, Phys. Rev. Lett. **31**, 121 (1973); Phys. Rep. **18**, 125 (1975).

[6] S. Krewald and J. Speth, Phys. Lett. B **52**, 295 (1974).

[7] M. Cavatino, M. Maragoni, and A. M. Saruis, Nucl. Phys. **A422**, 237 (1984).

[8] J. Ryckebusch, M. Waroquier, K. Heyde, J. Moreau, and D. Rychbosch, Nucl. Phys. **A476**, 237 (1988).

[9] P. Ring and P. Schuck, *The Nuclear Many-Body Problem*, (Springer-Verlag, New York, 1980).

[10] T. Udagawa and B. T. Kim, Phys. Rev. C **40**, 2271 (1989).

[11] B. T. Kim and T. Udagawa, Chinese J. Phys. **29**, 431 (1991).

[12] J. Y. Lee and B. T. Kim, J. Korean Phys. Soc. **29**, 588 (1996).

[13] J. Y. Lee, S. W. Hong, and B. T. Kim, J. Korean Phys. Soc. **33**, 388 (1998).

[14] M. C. Kyum, Ph. D. dissertation, Sungkyunkwan University (1996).

[15] T. Udagawa, S. W. Hong, and F. Osterfeld, Phys. Lett. B **245**, 1 (1990).

[16] T. Udagawa, P. Oltmanns, F. Osterfeld, and S. W. Hong, Phys. Rev. C **49**, 3162 (1994).

[17] A. N. Gorbunov and V. A. Osipova, JEPT (Sov. Phys.) **16**, 27 (1963).

[18] N. W. Tanner, G. C. Thomas and E. D. Earle, Nucl. Phys. **52**, 45 (1964).

[19] J. T. Caldwell *et al.*, University of California, Livermore preprint UCRL-12375 (1965).

[20] V. P. Denisov, A. P. Komar, and L. A. Kulchitsky, Nucl. Phys. **A113**, 289 (1968).

[21] D. E. Frederick, R. J. J. Sterart, and R. C. Morrison, Phys. Rev. **186**, 992 (1969).

[22] D. J. S. Findlay, thesis, Glasgow University (1975).

[23] D. J. S. Findlay and R. O. Owens, Nucl. Phys. **A279**, 385 (1977).

[24] B. Buck and A. D. Hill, Nucl. Phys. **A95**, 271 (1967).

[25] H. G. Wahsweiler, Walter Greiner, and Michael Danos, Phys. Rev. **170**, 893 (1968).

[26] H. Hebach, A. Wortberg, and M. Gari, Nucl. Phys. **A267**, 425 (1976).

[27] B. Schoch, Phys. Rev. Lett. **41**, 80 (1978).

[28] R. C. Morrison, thesis, Yale University Electron Accelerator Laboratory (1965).

[29] A. F. Khodjachikh, P. I. Vacet, I. V. Dogjust, and V. V. Kirichenko, Ukrains'Kii Fizichnit Zhurnal **25**, 229 (1980).

[30] R. R. Whitehead *et al.*, Adv. Nucl. Phys. **9**, 123 (1977).

[31] B. T. Kim, T. Udagawa, M. Benhamou, and T. Tamura, Phys. Rev. C **36**, 1270 (1986).

[32] W. G. Love, Nucl. Phys. **A312**, 160 (1978).